EXPLOITING PHOTONIC STRUCTURES TO IMPROVE THE EFFICIENCY OF UPCONVERSION BY FIELD ENHANCEMENT AND A MODIFICATION OF THE LOCAL DENSITY OF PHOTONIC STATES

S. Wolf[*1], B. Herter[*], S. Fischer[*], O. Höhn[*], R. Martín-Rodríguez[+], U. Aeberhard[°], J.C. Goldschmidt[*]
[*] Fraunhofer Institut für Solare Energiesysteme, Heidenhofstraße 2, 79110 Freiburg, Germany
[+] University of Utrecht, P.O. Box 80.000, 3508 TA Utrecht, Netherlands
[°] IEK-5 Photovoltaik, Forschungszentrum Jülich, 52425 Jülich, Germany
[1] phone: +49 761 4588 5762, fax: +49 761 4588 9520, email: sebastian.wolf@ise.faunhofer.de

ABSTRACT: Upconversion of infrared photons has been established as a concept to mitigate transmission losses in solar cells. Higher upconversion efficiencies, however, are necessary, to enable a profitable application of upconverting components. In this paper, we examine the embedding of upconverting material into a photonic structure to increase upconversion efficiencies. The structure influences the upconversion efficiency in two ways: First, higher local field intensities increase the absorption and the population of higher excited states. Second, the local density of photonic states is modified by the structure. Thus, the probabilities of desired transitions can be increased. This work covers the design of a suitable model structure and its examination via various simulation methods, most importantly finite-difference time-domain simulations, combined with an upconverter rate-equation model. An increase of the upconversion efficiency by a factor of about 3.6 at an excitation irradiance of 200 Wm^{-2} is determined.

Keywords: Upconversion, Photonic Structures, Simulation

1 INTRODUCTION

The theoretical efficiency of a semiconductor solar cell is limited by two loss mechanisms related to the semiconductor's band gap. Part of the energy of high-energy photons is lost in thermalization processes of the hot charge carriers. Photons with energies below the band gap, on the other hand, are not absorbed by the semiconductor. The theoretical limit for a conventional silicon solar cell has been calculated by Shockley and Queisser to be about 30 % [1]. The losses due to transmission of the low energy photons account for approximately 20 % of the energy contained in the incident solar *AM1.5G* spectrum.

An upconverter behind a bifacial solar cell can utilize this transmitted light to generate higher-energy photons out of two or more low-energy photons. The upconverted light can subsequently be used by the solar cell, allowing theoretical efficiencies beyond the Shockley-Queisser limit of up to 40 % for a silicon solar cell under non-concentrated illumination [3].

Trivalent rare earth ions in host crystals are well known to support upconverison of near infrared (NIR) photons. Among the rare earth ions, the trivalent erbium ion shows especially suitable properties for the application in silicon solar cell systems. The basic excitation wavelength in Er^{3+} lies at around 1523 nm, as the corresponding energy can excite the first transition from the ground state to the first excited state as well as transitions between higher levels. (In this paper, all denoted wavelengths refer to the respective vacuum wavelength.) The strongest transition for use in a silicon solar cell is the spontaneous emission from $^4I_{11/2}$ to $^4I_{15/2}$ with a wavelength of about 980 nm (see Figure 1).

Up to now, achieved upconversion efficiencies are too low, to make the application of upconversion economically attractive in the context of photovoltaics [4]. Therefore, different concepts are investigated to increase upconversion efficiencies. The first approach is to increase the irradiance of the excitation: Different competing and interacting processes can lead to upconversion [5]. All of them require the absorption of at least two photons in a short time interval in a small volume. Therefore, upconversion is a non-linear process and its efficiency increases with the excitation irradiance. Figure 2 shows this dependence on the basis of experimental results for the upconverter material β-$NaY_{0.8}F_4$:20%Er^{3+}.

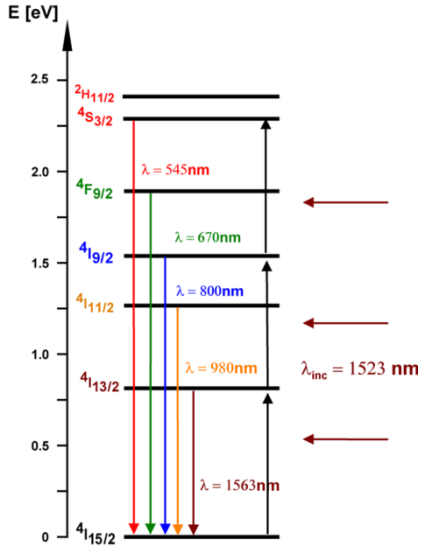

Figure 1: Energy levels of erbium in the β-$NaY_{0.8}F_4$:20%Er^{3+} system, with the corresponding emission wavelengths to the ground state. Furthermore, the transitions that can be excited monochromatically with a wavelength of 1523 nm are indicated. [2]

Ways to increase the irradiance are external concentration with lenses or mirrors, and the use of a second luminescent material that extends the used spectral range [6], which can be additionally used to form a luminescent concentrator [7]. Every upconversion process naturally consists of a chain of transitions in one or between several ions. Thus, the overall upconversion efficiency also depends on the probability of the involved individual

transitions.

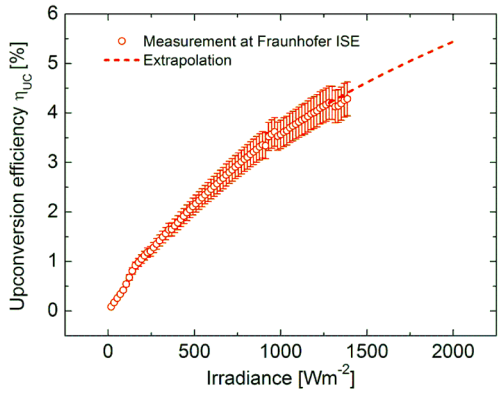

Figure 2: Measured optical efficiency of β-$NaY_{0.8}F_4$:20%Er^{3+} over the excitation irradianceat monochromatic illumination. The efficiency depends strongly on the irradiance [8]. This dependence can be described by a power law, as shown in the graph.

Plasmonic resonance in metallic nanoparticles in the vicinity of the upconverter can affect both the local irradiance of the excitation and the probability of the individual transitions [9-12]. In this paper, we present another concept: Dielectric photonic structures can as well increase the local irradiance and modify the probability of the individual transitions. If carefully designed, both effects can be used to increase upconversion efficiency without the significant absorption losses, plasmonic concepts are prone to. First, we present the special configuration of photonic structures investigated in this paper, then we give an overview over the used simulation methods. A transfer matrix approach is used to optimize components of the investigated structure. The optical properties of the overall structure are further determined using finite-difference time-domain (FDTD) simulations. These data serve as an input for a rate equation model of the upconversion. Finally, we present and analyze the obtained results for the achievable increase in upconversion efficiency.

2 INVESTIGATED STRUCTURE

As a model system for a dielectric photonic structure, we investigate a layer containing the upconverter β-$NaY_{0.8}F_4$:20%Er^{3+} embedded into a dielectric multilayer structure (see Figure 3). The multilayer stacks act as highly wavelength-selective filters. With a proper design of the surrounding filters, the upconverter layer becomes a high-quality cavity, resonant at the desired emission wavelength λ_{em} = 980 nm. The intention is to make use of the Purcell Effect [13], which increases spontaneous emission in a resonant environment due to a modification of the local density of photonic states (LDOS). Thus, the spontaneous emission out of $^4I_{11/2}$ to $^4I_{15/2}$ can be favored over competing transitions, leading to a higher yield in upconverted photons. A similar design has been proposed in [14] to enhance the emission from $^4I_{13/2}$.

We assume a monochromatic plane wave excitation from the top with an excitation wavelength λ_{exc} = 1523 nm. Therefore, the filters surrounding the cavity should show complete transmission at λ_{exc}. To increase the irradiance of the excitation in the cavity, an additional third filter, showing high reflection at λ_{exc}, is placed at the rear of the structure, separated by a buffer layer.

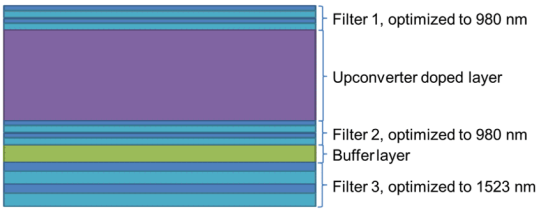

Figure 3: Cross section through the proposed structure. The filter elements are only shown schematically and actually consist of several more layers of alternating refractive index. The given wavelengths indicate the region, in which high reflection is achieved. Not shown are the considered superstrate and substrate simulated as glass.

3 SIMULATION METHODS

Since the reflectivity of the Filter 1 on top of the cavity needs to be very high around λ_{em} but as low as possible at λ_{exc}, the specific filter design has to be optimized to meet these specifications. Based on a regular Bragg reflector design, the filters to be adapted consist of multiple stacked layers with two alternating refractive indices n_{high} and n_{low}. In a conventional Bragg reflector the layer thickness is given as $\delta_i = \lambda_c/(4n_i)$,where λ_c is the wavelength of maximum reflectivity.

First, the outer layers were replaced by δ_i /2 layers to mitigate side band reflectivity, as described in [15]. Then single layer thicknesses were optimized, using a genetic algorithm. By mutation and crossing, individual layer thicknesses were varied, and the resulting reflection spectrum calculated with the transfer matrix method [15]. The obtained reflectivity is valuated according a fitness function that weights the averaged reflection in the desired wavelength range against reflection in an undesired range. The fittest structures were then further mutated. Using the algorithm for 200 generations, a filter structure with the desired properties could be found.

The optimized filter structure was subsequently implemented into a FDTD simulation of the complete system shown in Figure 3 [16].

The final outcome of the simulations is the efficiency η_{UC} of the radiative transition from $^4I_{11/2}$ to $^4I_{15/2}$ in the upconverter embedded in the structure, which is defined by

$$\eta_{UC} = \frac{Lum_{tot}}{Abs_{tot}}. \qquad (1)$$

The total luminescence Lum_{tot} and absorption Abs_{tot} for a given excitation irradiance are calculated by a rate-equation model of the upconverter [17].The input data for the rate equation model are the spatially resolved data of the change in the irradiance and of the change in the probabilities of all included transitions. Both data sets can be obtained from FDTD simulations of the structures.

The first step is to determine the change of irradiance in the structure. It is assumed, that the structure

influences incident light independent of its intensity. Therefore, only the local enhancement factor of irradiance γ_E is of interest, which compares the irradiance at a certain point $I_{struct}(\boldsymbol{r})$ to the case $I_0(\boldsymbol{r})$ without the structure in a homogeneous medium of same refractive index as the cavity layer. One can express the factor in terms of the electric fields $E_{struct}(\boldsymbol{r})$ in the structure, and $E_0(\boldsymbol{r})$ in the reference respectively:

$$\gamma_E(\boldsymbol{r}) = \langle \frac{I_{struct}(\boldsymbol{r})}{I_0(\boldsymbol{r})} \rangle_t = \langle \left(\frac{E_{struct}(\boldsymbol{r})}{E_0(\boldsymbol{r})} \right)^2 \rangle_t \,. \qquad (2)$$

As put here, we are only interested in the time-averaged values of the irradiance. The program used for the FDTD implementation supports the calculation of complex fields. This is useful, because the length of the complex field vector is proportional to the time-average of the real field amplitude in each point of space [16]. With these considerations, the irradiance enhancement is calculated by

$$\gamma_E(\boldsymbol{r}) = \left(\frac{|E_{struct}(\boldsymbol{r})|}{|E_0(\boldsymbol{r})|} \right)^2 , \qquad (3)$$

with $E_{struct}, E_0 \in \mathbb{C}$.

With the simulated plane wave illumination from the top of the simulation cell, the investigated structure represents a one-dimensional problem. Therefore, the simulation cell can be reduced to just one coordinate. The fields are recorded once the steady-state field distribution is reached after the plane wave illumination has been switched on. It has to be noted that all simulations are carried out under the approximation that the absorption in the cavity layer is negligible.

Secondly, the influence of the structure on the transition probabilities in the upconverter must be determined. The transition probabilities can be expressed by the Einstein coefficients B_{if} for absorption and B_{fi} for stimulated emission and A_{fi} for spontaneous emission [18]. The probability for absorption P_{if} is given by the product of the Einstein coefficient and the spectral energy density $u(\nu)$:

$$P_{if} = u(\nu_{if}) B_{if} \,, \qquad (4)$$

while the probability for spontaneous emission $P_{fi,SE}$ is

$$P_{fi,SE} = A_{fi} \,. \qquad (5)$$

In the case without degeneration of the energy levels, it is $B_{if} = B_{fi}$. These coefficients are material properties, while A_{fi} is linked to B_{fi} by the relation

$$A_{fi} = \rho(\boldsymbol{r}, \nu_{if}) B_{fi} \,, \qquad (6)$$

with $\rho(r,\nu_{if})$ being the local density of photonic states (LDOS). This shows that the probability of spontaneous emission can be adjusted by altering the LDOS.

To determine the change factor γ_{if} of the LDOS due to the photonic structure at the transition frequencies, in the FDTD simulation, the source outside of the structure is replaced by a point sized dipole emitter within the cavity layer. This source is set to emit a light pulse with a Gaussian spectral shape. That way, a certain frequency range can be covered with a single simulation. Over the pulse duration, the dipole radiates an amount of energy proportional to the local density of photonic states.

The emitted energy is measured as the waves pass through a box of detector planes surrounding the source. In these flux planes, the Fourier transform of the passing waves is calculated. Thus, after the simulation run, the emitted energy is obtained spectrally resolved. By dividing the deformed Gauss shape by the corresponding unperturbed values taken from a reference simulation in a homogeneous medium, the modified emission probabilities γ_{if} for radiant transitions from state i to state f is obtained, which correspond to a locally altered DOS:

$$\gamma_{if} = \frac{W_{struct}(\nu_{if})}{W_0(\nu_{if})} , \qquad (7)$$

where the energy

$$W(\nu_{if}) = \int_{\Delta T} \int_{A'} \left. \frac{\partial \boldsymbol{S}}{\partial \nu} \right|_{\nu_{if}} \Delta\nu \cdot d\boldsymbol{A} dt \qquad (8)$$

is the respective spectral fraction of the Poynting vector $\boldsymbol{S}$ in the transition frequency interval $\Delta\nu$ around ν_{if}, integrated over the flux detection planes of area A' and the measurement time ΔT. In principle, this method has been demonstrated in [19].

Again, the homogenous medium in the reference simulations is set to the same refractive index as the cavity layer in the structure, since the emitted power of the dipole scales with this property.

Contrary to the above irradiance simulations, this case cannot simply be treated as a one dimensional problem, as the dipole radiates in all directions except along its axis. Since both directions parallel to the layer planes are equivalent, simulations can be executed in a two-dimensional cross section plane as suggested in Figure 3. By doing this, the computational effort can be greatly decreased. The obtained change factors, however, are only qualitatively correct, as both parallel directions would have to be weighted against the direction perpendicular to the planes for an absolute view of the case. Since any direction parallel to the layer planes are equivalent, though, no qualitative change is to be expected here. This simulation is repeated for 49 raster positions on a vertical line throughout the cavity layer to obtain the spatially resolved change of the LDOS.

The two sets of data obtained from the simulations, the local irradiance change γ_E and the change values for the coefficients of spontaneous emission γ_{if} are then integrated into the rate model. The model has been adjusted to describe the dynamics of the β-$NaY_{0.8}F_4$:20%Er^{3+} upconverter system. It is implemented as a set of differential equations in matrix form that describe the populations and transition rates of the six lowest states in the Er^{3+} ion. The model is described in detail in [17]. Based on the input data, the absorption and luminescence rates, as well as the derived efficiencies for the single transitions can be calculated for a given excitation irradiance and compared with the values based on a homogeneous medium.

4 RESULTS AND DISCUSSION

As described before, the filter designs were obtained from an optimization algorithm. The chosen design for the filters around the cavity consists of 17 alternating layers. This design is used for both Filters 1 and 2. The rear reflector, Filter 3, comprises 21 layers. The interchanging refractive indices of the layers are $n_{high} = 2.5$ and $n_{low} = 1.8$ respectively. The resulting

reflection spectra are shown in Figure 4. The calculated reflectivities are 97.3% at 980 nm and 0.004% at 1523 nm on Filters 1 and 2, while Filter 3 gives a 98.9% reflectivity at 1523 nm.

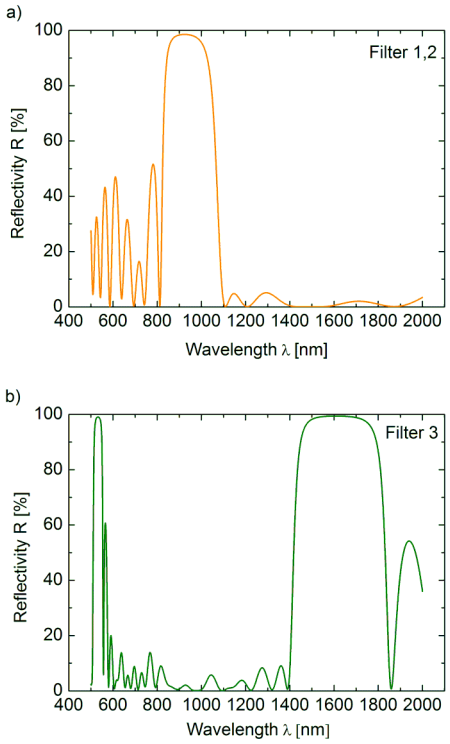

Figure 4: Calculated spectral reflectivity **a)** of the dielectric Filters 1 and 2 around the cavity and **b)** of Filter 3 at the rear.

The obtained layer thicknesses were used for the geometric specifications of the FDTD simulations. In a series of simulation runs, the thickness d of the cavity layer was varied in a range between 100 nm and 915 nm. This was done for both the irradiance simulations with external light source and the emission simulations with the source inside the structure. Figure 5 shows an example of the field enhancement in the structure. It can be seen that the rear reflector works effectively on the excitation wavelength and creates an interference pattern inside the structure.

As a result of this thickness variation favorable values for the cavity layer thickness regarding the irradiance enhancement distribution could be found. Around $d = 790$ nm, the cavity contains two maxima of the field enhancement but only one minimum. As the filters surrounding the cavity are highly transparent to λ_{exc}, this is not an effect of the cavity, though. Instead it results only from the position of the cavity with respect to the rear reflector.

In the simulations with the emitter inside the photonic structure, the cavity layer was scanned in steps of 2% of the layer thickness for each variation. Thus, a map for the changes of the transition rates for spontaneous emission was created for each layer thickness. An exemplary map is shown in Figure 6.

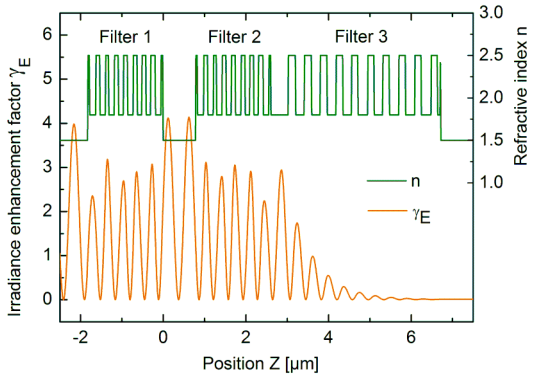

Figure 5: Irradiance enhancement γ_E over position in the structure for a cavity thickness $d = 790$ nm. For orientation, the implemented refractive index structure is shown as well. The cavity is represented by the area of $n = 1.5$ between Filter 1 and 2. The interference pattern with two maxima in the cavity is visible as well as the exponential decay of the fields in the rear reflector.

In the variations of the cavity layer thickness, a characteristic resonance pattern was observed. It features one- to fourfold resonance peaks that shift towards longer wavelengths for a wider cavity. As effect of the resonance, the change of transition rates is the highest in the high reflection range of the surrounding filters. In expectation of a favorable resonance position, 10 nm variation steps were used between 750 nm and 900 nm for the cavity layer thickness. For $d = 790$ nm, the maximum of the two peak resonance lies directly at 980 nm (see Figure 6).

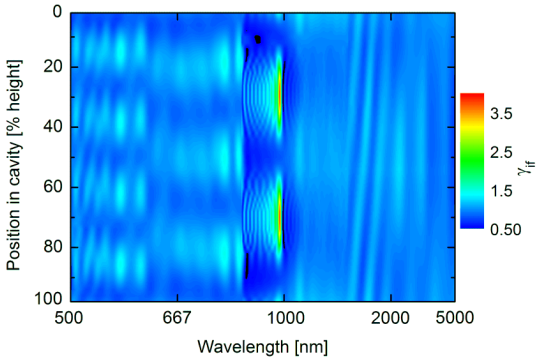

Figure 6: Map of the changes in the spontaneous emission probability γ_{if}. The vertical coordinate denotes the dipole position in the cavity while the horizontal direction shows the wavelengths of a potential transition on a reciprocal scale. The cavity thickness is $d = 790$ nm, which leads to a strong two-peak resonance in the LDOS at λ_{em}=980 nm.

For each variation, the data was evaluated by calculating the resulting absorption of incident photons with a wavelength of λ_{exc}=1523 nm and the luminescence at λ_{em}=980 nm according to the rate equation model on every sampling point in the cavity layer. The values were then compared to the rate equation model applied to an upconverter in a homogeneous medium. Figure 7 shows the resulting mean enhancements depending on the cavity layer thickness d.

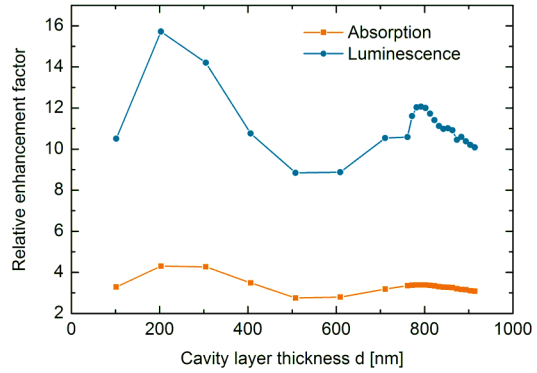

Figure 7: Mean absorption and luminescence enhancement by the structure over the cavity thickness. An external excitation irradiance of $I_{exc} = 200\ \mathrm{Wm^{-2}}$ was assumed.

From these values, the upconcversion efficiency enhancement due to the photonic structure was calculated as defined in Equation (1). These results are shown in Figure 8.

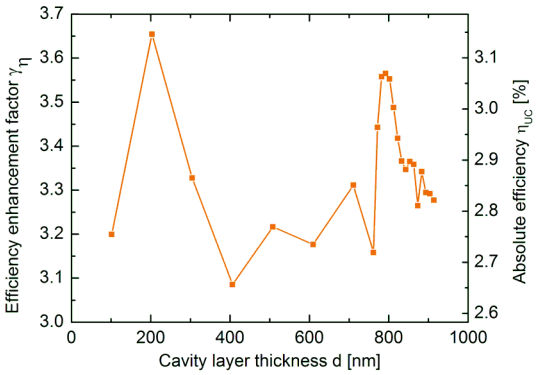

Figure 8: Relative change factor γ_η of the upconversion efficiency η_{UC} caused by the structure (left scale) and the corresponding absolute values (right scale), assuming an external excitation with $I_{exc} = 200\ \mathrm{Wm^{-2}}$.

The values show that the structure has the potential to significantly increase the efficiency of an embedded upconverter, by a factor of more than 3.6 at an irradiance of $200\ \mathrm{Wm^{-2}}$. The overall upconversion efficiency strongly depends on the irradiance I_{exc}. Higher absolute efficiencies can be achieved with higher irradiance values. At an excitation irradiance of $1880\ \mathrm{Wm^{-2}}$, an efficiency of $\eta_{UC} = 9.9\%$ was calculated. This means an increase by the factor $\gamma_\eta = 1.9$ in comparison to the data shown in Figure 2. The efficiency change factor achieved by the structure decreases due to the slight saturation in the dependence on the irradiance visible in Figure 2.
A matter of interest is still to what effect the increase can be mainly attributed. Figure 7 shows the luminescence change roughly following the square of the absorption. Deviations caused by an altered LDOS are clearly visible, but not predominant. A control calculation without taking altered transition coefficients shows that without the modification of the LDOS the overall efficiency would be higher (see Figure 9). That is, the main source of the increase in efficiency is the change of the excitation irradiance, while the modification of the transition rates actually decreases the efficiency.

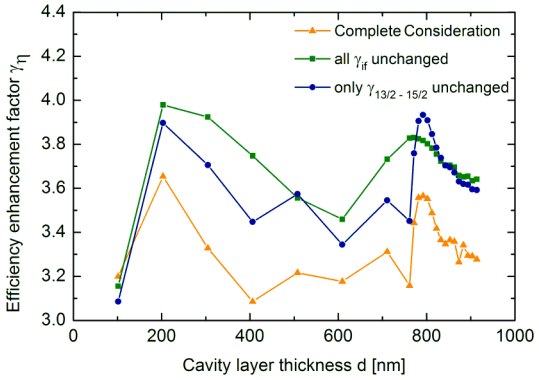

Figure 9: The change of the efficiency γ_η in dependence of the cavity layer thickness d for different assumptions for the change of the transitions rates. The squares represent the case for all relevant changes of the transitions taken into account (as already presented in Figure 8) in comparison to two hypothetical calculations. The green curve with the triangles shows a calculation without altered A_{if}. In the blue curve with the circles, only the changes in the transition coefficient $A_{13/2\text{-}15/2}$ were neglected. This transition represents the direct de-excitation of the first excited level via spontaneous emission.

The presumed reason for this negative effect of the changed transition rates is that the transition probability at λ_{exc}, although only slightly changed, leads to an increased depopulation of $^4I_{13/2}$ in the respective areas of the structure. The presumption is backed by the observation that the absorption from $^4I_{15/2}$ is weakly increased in the calculation with altered transition coefficients. This is evidence for a higher average ground state population originating from a higher repopulation rate. That way, luminescence from higher levels is rather quenched because the excited state absorption rate out of $^4I_{13/2}$ is decreased.
If one considers the changed coefficients A_{if} for all but the lowest transition, as shown in the blue curve with the spheres, it can be seen, that the efficiency increases, which supports the presented explanation. For some layer thicknesses, the values from the calculation with selectively changed emission probabilities are even higher than the curve without any modification. This opens the perspective to further increase the positive impact of the structure by finding a design, in which the increase in the wanted emission probabilities can be uncoupled from the change of the emission for the lowest transition.

5 CONCLUSION AND OUTLOOK

A model structure aiming to increase the efficiency of an embedded upconverter was designed. By finite-difference time-domain simulations, the effect of the structure on the internal irradiance distribution as well as the local density of photonic states was examined over variations of the cavity layer thickness. The results of these simulations were fundamental for further calculations to determine the direct effect on an embedded upconverter. We have shown that such a structure can significantly increase the upconversion efficiency. Upconversion efficiencies of more than 3 % for an external excitation irradiance of 200 W/m² have

been determined. This corresponds to a relative efficiency enhancement of a factor of more than 3.5. This increase is mainly due to an increased absorption by the upconverter. The modification of the local density of photon states (LDOS) shows significant effect on the luminescence from $^4I_{11/2}$. Unfortunately, the overall effect of a modified LDOS has so far been counterproductive, as the higher states get populated less in the first place.
Further research needs to show whether the LDOS can be altered more specifically, such that only wanted de-excitation processes are amplified. So far, the results of this idealized model are of hypothetical nature. To obtain sound conclusions, a more realistic analysis of the system is needed. For this, also the effects of absorption and re-emission on the field distributions at λ_{exc} have to be taken into account, as well as the potential of stimulated emission at λ_{em}.
For an experimental examination of the case, the model structure is to be built according to the found proportions. The filters can be realized by multilayer SiC structures, fabricated by PECVD. For the cavity layer, nanocrystalline Er^{3+}-doped particles in a polymer matrix are considered, since the grain size of conventional powder samples of upconverter material exceed the needed dimensions.

6 ACKNOWLEDGEMENTS

The research leading to these results has received funding from the European Community's Seventh Framework Programme (FP7/2007-2013) under grant agreement n° [246200]. S. Fischer and O. Höhn gratefully acknowledge the scholarship support from the Deutsche Bundesstiftung Umwelt DBU.

6 REFERENCES

[1] Shockley, W. and H.J. Queisser, *Detailed balance limit of efficiency of p-n junction solar cells.* Journal of Applied Physics, 1961. **32**(3): p. 510-9.
[2] Goldschmidt, J.C., *Novel solar cell concepts*. 2010, München: Verlag Dr. Hut. 280.
[3] Trupke, T., M.A. Green, and P. Würfel, *Improving solar cell efficiencies by up-conversion of sub-band-gap light.* Journal of Applied Physics, 2002. **92**(7): p. 4117-22.
[4] Goldschmidt, J.C., et al., *Experimental analysis of upconversion with both coherent monochromatic irradiation and broad spectrum illumination.* Solar Energy Materials and Solar Cells, 2011. **95**(7): p. 1960-3.
[5] Auzel, F., *Upconversion and anti-stokes processes with f and d ions in solids.* Chemical Review, 2004. **104**: p. 139-73.
[6] Strümpel, C., et al. *Erbium-doped up-converters of silicon solar cells: assessment of the potential*. in *Proceedings of the 20th European Photovoltaic Solar Energy Conference*. 2005. Barcelona, Spain.
[7] Goldschmidt, J.C., et al. *Advanced Upconverter Systems with Spectral and Geometric Concentration for high Upconversion Efficiencies*. in *Proceedings IUMRS International Conference on Electronic Materials*. 2008. Sydney, Australia.
[8] Fischer, S., et al., *Enhancement of silicon solar cell efficiency by upconversion: Optical and electrical characterization.* Journal of Applied Physics, 2010. **108**(4): p. 044912.
[9] Fischer, S., et al., *Plasmon enhanced upconversion luminescence near gold nanoparticles - simulation and analysis of the interactions.* Optics Express, 2012. **20**(1): p. 271-82.
[10] Hallermann, F., et al., *On the use of localized plasmon polaritons in solar cells.* Physica Status Solidi A, 2008. **205**(12): p. 2844-61.
[11] Goldschmidt, J.C., et al., *Increasing upconversion by plasmon resonance in metal nanoparticles - a combined simulation analysis.* IEEE Journal of Photovoltaics, 2012. **2**(2): p. 134-40.
[12] Goldschmidt, J.C., et al. *Increasing upconversion by metal and dielectric nanostructures*. in *Proceedings of SPIE*. 2012. San Francisco, California, USA: SPIE.
[13] Purcell, E.M., *Spontaneous emission probabilities at radio frequencies.* Physical Review, 1946. **69**: p. 681.
[14] Lopez, H.A. and P.M. Fauchet, *Erbium emission from porous silicon one-dimensional photonic band gap structures.* Applied Physics Letters, 2000. **77**(23): p. 3704-3706.
[15] Macleod, H.A., *Thin film optical filters*. 3rd ed. 2001: Taylor & Francis. 668.
[16] Oskooi, A.F., et al., *MEEP: a flexible free-software package for electromagnetic simulations by the FDTD method.* Computer Physics Communications, 2010. **181**(3): p. 687-702.
[17] Fischer, S., et al., *Modeling upconversion of erbium doped microcrystals based on experimentally determined Einstein coefficients.* Journal of Applied Physics, 2012. **111**: p. 013109.
[18] Einstein, A., *Zur Quantentheorie der Strahlung.* Physikalische Zeitschrift, 1917. **18**: p. 121-8.
[19] Bermel, P., et al., *Tailoring Optical Nonlinearities via the Purcell Effect.* Phys. Rev. Lett., 2007. **99**: p. 053601.